Highly Conductive Boron Nanotubes: Transport Properties, Work Functions, and Structural Stabilities

Viktor Bezugly,[†,*] Jens Kunstmann,[†] Bernhard Grundkötter-Stock,[‡] Thomas Frauenheim,[‡] Thomas Niehaus,[§] and Gianaurelio Cuniberti[†,⊥]

[†]Institute for Materials Science and Max Bergmann Center of Biomaterials, Dresden University of Technology, 01062 Dresden, Germany, [‡]Bremen Center for Computational Materials Science, Universität Bremen, Am Fallturm 1, 28359 Bremen, Germany, [§]University of Regensburg, 93040 Regensburg, Germany, and [⊥]Division of IT Convergence Engineering, POSTECH, Pohang 790-784, Republic of Korea

ABSTRACT The transport properties, work functions, electronic structure, and structural stability of boron nanotubes with different lattice structures, radii, and chiralities are investigated theoretically. As the atomic structure of boron nanotubes and the related sheets is still under debate, three probable structural classes (nanotubes derived from the α-sheet, the buckled triangular sheet, and the distorted hexagonal sheet) are considered. For comparison with recent transport measurements [*J. Mater. Chem.* 2010, *20*, 2197], the intrinsic conductance of ideal nanotubes with large diameters ($D \approx 10$ nm) is determined. All considered boron nanotubes are highly conductive, irrespective of their lattice structures and chiralities, and they have higher conductivities than carbon nanotubes. Furthermore, the work functions of the three sheets and the corresponding large-diameter nanotubes are determined. It is found that the value of the nanotubes obtained from the α-sheet agrees well with the experiment. This indirectly shows that the atomic structure of boron nanotubes is related to the α-sheet. The structural stability of nanotubes with diameters > 2 nm approaches that of the corresponding boron sheets, and α-sheet nanotubes are the most stable ones. However, for smaller diameters the relative stabilities change significantly, and for diameters < 0.5 nm the most stable structures are zigzag nanotubes of the buckled triangular sheet. For structures related to the distorted hexagonal sheet the most stable nanotube is discovered to have a diameter of 0.39 nm.

KEYWORDS: nanotubes · boron · structural stability · electronic properties · work function · ballistic transport · *ab initio* calculations

Carbon nanotubes (CNTs) and graphene, the low-dimensional structures of elemental carbon, are of great interest to the scientific community.[2,3] This is not only because of their unique physical properties but also because of their potential use in nanoscale devices. However, future nanotechnologies cannot be realized with carbon allotropes only. In order to develop technologies a variety of materials with different basic properties are needed. In the quest for new materials, the interest in elemental boron, the neighbor of carbon in the periodic table, has always been high and led to the recent discovery of a new bulk phase.[4] The hope to find boron nanostructures similar to graphene and CNTs arose after the prediction of stable, quasi-planar, and tubular clusters of elemental boron,[5,6] which was later confirmed experimentally.[7−9] Treating these quasiplanar boron clusters as embryos of boron sheets and nanotubes, several models of stable boron nanostructures with different underlying lattices have been proposed.[10−15] Finally, Ciuparu *et al.* and Liu *et al.* reported the first successes in growing pure boron nanotubes (BNTs).[1,16]

However, the atomic structure of these BNTs is still unclear, because the quasi two-dimensional sheet that constitutes the walls of BNTs has not yet been experimentally discovered. So far several models of stable boron sheets have been proposed, which fall into three structural classes: triangular, hexagonal, and mixed triangular−hexagonal structures. In order to obtain unbiased results we study BNTs derived from one favorable representative of each class,[17] *i.e.*, the buckled triangular (BT) sheet,[15] the distorted hexagonal (DH) sheet,[11] and the so-called α-sheet.[12] It is well known that boron exhibits a pronounced polymorphism. Hence, it is possible that not only one but multiple sheet structures are realized in nature. Therefore, we first compare the basic structural stability of different BNTs and calculate cohesive energies and strain energies of a set of nanotubes from each of these three structural classes.

It is well known that carbon nanotubes can be either metallic or semiconducting depending on their diameter and the chiral angle. However, it is still a challenge to produce CNTs with well-defined electronic properties. Because of these (and other) difficulties, CNTs are not yet used in current technologies. In contrast to carbon nanotubes, BNTs of all structural classes are

* Address correspondence to Viktor.Bezugly@tu-dresden.de.

Received for review March 23, 2011 and accepted April 29, 2011.

Published online April 29, 2011
10.1021/nn201099a

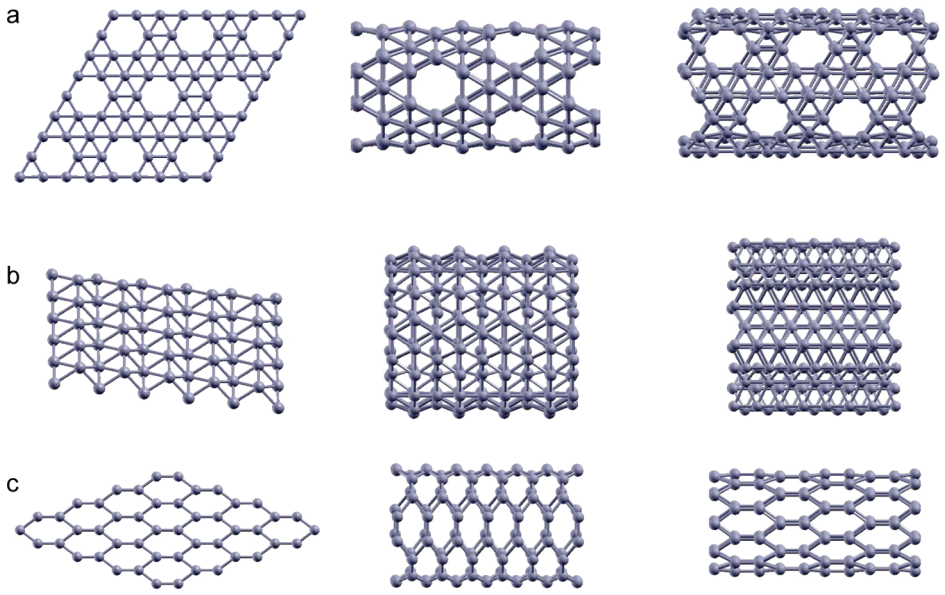

Figure 1. Atomic structure of boron sheets (first column) and armchair and zigzag boron nanotubes (second and third columns, respectively). (a) Structures derived from the α-sheet, (b) the buckled triangular (BT) sheet, and (c) the distorted hexagonal (DH) sheet. As the atomic structure of boron nanotubes is not definitely known, we consider the three most probable structure models (a−c) for the calculation of physical properties.

predicted to be metallic only, irrespective of their diameters and chiral angles.[10,11,15,18] For small-diameter BNTs based on the α-sheet (diameter <1.7 nm), density functional theory (DFT) calculations predict that the nanotubes are semiconducting due to a curvature-induced slight out-of-plane buckling of certain atoms.[13,14,41] However, recent calculations at higher levels of theory (MP2) indicate that the buckling might be an artifact of DFT.[18] Without buckling, all BNTs based on the α-sheet are metallic. This feature could make BNTs excellent candidates for future nanometer-scale conducting elements. Recently Liu *et al.* reported conductivity measurements on large-diameter (10 to 40 nm) multiwalled BNTs that confirmed this prediction.[1] Theoretical investigations of electron transport through boron nanostructures were done only for fullerene-like[19] and flat[20,21] boron clusters as well as small-radius boron nanotubes.[22,23] To allow for a comparison with the experiments of Liu *et al.*, we calculate the electronic structure and transport properties of BNTs with diameters of approximately 10 nm. Again we consider BNTs from each of the three structural classes. We further calculate the work functions of the three boron sheets and find that the one of the α-sheet agrees well with the measurements of Liu *et al.*[1]

RESULTS AND DISCUSSION

Atomic Structures. As the atomic structure of BNTs is not definitely known, one has to consider different structural models for the calculation of physical properties. In the present work, armchair and zigzag BNTs derived from the three most stable boron sheets are considered. These are the so-called α-sheet, the buckled triangular sheet, and the distorted hexagonal sheet. The atomic structures of the boron sheets and armchair and zigzag BNTs are shown in Figure 1. In the following text the BNTs are denoted with respect to the boron sheet they originate from and the direction in which they are rolled as "α-BNT arm", "α-BNT zz" (Figure 1a), "BT-BNT arm", "BT-BNT zz" (Figure 1b), "DH-BNT arm", and "DH-BNT zz" (Figure 1c). For the detailed geometries of the sheets (lattice vectors and atomic position) and the definition of the chiral vector for a specific (*n*,*m*) nanotube, see the Supporting Information.

Structural Stabilities. First the cohesive energies E^{coh} and the strain energies E^{st} of small-diameter BNTs are studied. The cohesive energy (also known as binding energy or atomization energy) of a system is defined as $E^{coh} = -E^{tot}/N + E^{at}$, where E^{tot} and E^{at} are the ground-state energies of the whole system and an isolated boron atom, respectively, and N is the number of atoms in the system. From this definition it follows that positive values of E^{coh} correspond to bound (stable) structures. To a first approximation, the chemical stability of a certain structure can be judged by E^{coh}. The ground-state energies are calculated with density functional theory using the PBE exchange−correlation functional,[24] and the geometries of all considered structures were fully optimized. The cohesive energies of the three boron sheets and of different BNTs with diameters D up to 2.3 nm are shown in Figure 2a. For BT-BNTs D is defined as the average between the inner and the outer diameter of a tube.

The relative stabilities of the boron sheets presented here are in agreement with the literature;[17] that is, the α-sheet is the most stable structure and the DH sheet is the least stable one, and the BT sheet has an

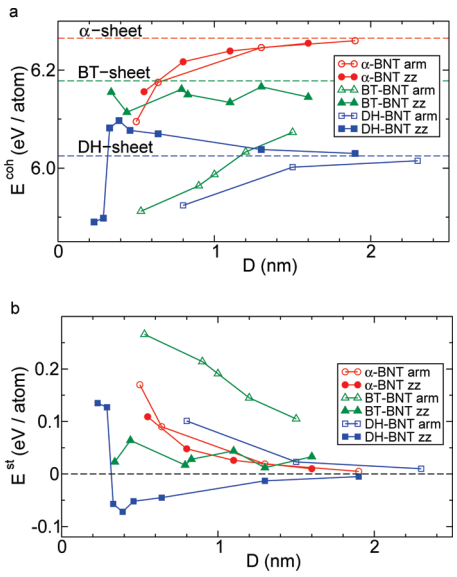

Figure 2. Cohesive energies and strain energies of small-diameter armchair (arm) and zigzag (zz) boron nanotubes of different structural classes. (a) For nanotubes with $D > 2$ nm their relative stabilities approach those of the corresponding boron sheets (dashed lines); however for $D < 2$ nm the relative stabilities change significantly, and for $D < 0.5$ nm α-BNTs are no longer the most stable structures, but rather BT-BNT zz are now more stable. The cohesive energy of DH-BNT zz systems has a maximum at $D = 0.39$ nm, corresponding to the (6,−6) DH-BNT zz nanotube. The latter is the most stable structure of the distorted hexagonal family. (b) The strain energy of a boron nanotube depends on both diameter and chirality; for α-BNTs it depends only on the diameter. DH-BNT zz systems have negative strain energies (except of the two smallest ones), which means that small-diameter DH-BNT zz nanotubes are particularly stable.

intermediate energy (their cohesive energies are 6.27, 6.03, and 6.18 eV/atom, respectively). For large diameters the curvature effects of BNTs are small and E^{coh} of all BNTs approaches the value of the corresponding boron sheet. However for tubes with diameters less than about 2 nm the relative stabilities of the three structural classes change significantly. In Figure 2a one sees two intersections of curves: α-BNTs with BT-BNT zz at $D \approx 0.5$ nm and DH-BNT zz with BT-BNT arm at $D \approx 1.25$ nm, indicating that at these points the relative stability of two classes changes sign. It follows that for diameters $D < 0.5$ nm, the α-BNT are no longer the most stable structures, but rather BT-BNT zz becomes more stable.

Furthermore, we discovered that E^{coh} for DH-BNT zz systems goes through a maximum at $D = 0.39$ nm followed by a sudden drop. The maximum corresponds to the (6,−6) DH-BNT zz nanotube (for illustration of its atomic structure see the Supporting Information), which is the most stable structure of the distorted hexagonal family. To our knowledge, there is no other nanotubular system reported in the literature that forms one tube that is energetically favored over all other tubes.

The end points of the lines for DH-BNT zz and BT-BNT zz correspond to the smallest possible structures of that class: a (3,−3) DH-BNT zz studied earlier by Zhang *et al.*[25] and a (3,0) BT-BNT zz that can be seen as the periodically continued toroidal part of a B_{12} icosahedron. Among the boron nanotubes with the smallest diameters, the (3,0) BT-BNT zz is the most stable one. The particular stability of the (3,0) BT-BNT zz tube was first shown by Boustani *et al.* for small clusters.[26,27] These original results are the foundation of the whole field of boron nanostructures.

The strain energy (also known as curvature energy) as shown in Figure 2b is the amount of energy (per atom) needed to roll up a flat sheet into a specific (n,m) nanotube. It is defined as the difference between the cohesive energies of the sheet and the nanotube: $E^{st} = E^{coh}_{BS} - E^{coh}_{BNT}$. As already mentioned above, the curvature effects decrease with increasing diameter, and therefore E^{st} tends to zero for BNTs with large diameters. The strain energies of both armchair and zigzag types of α-BNTs lie essentially on one line and they follow the $E^{st} = C/D^2$ law known from elasticity theory.[28] By fitting the data points in Figure 2b, one obtains $C = 0.0352$ eV nm^2/atom, which agrees well with the value $C = 0.0364$ eV nm^2/atom obtained by Sign *et al.* with DFT/PBE calculations.[13] A very different behavior is found for BT-BNTs and DH-BNTs where E^{st} depends not only on the tube's diameter but also on its chirality; that is, in Figure 2b armchair and zigzag BNTs of these classes follow a different trend. This behavior can be ascribed to anisotropic in-plane mechanical properties of the corresponding boron sheets, and rolling up the sheet to nanotubes with similar diameters but along different in-plane lattice directions (chiralities) leads to different strain energies. This effect was discussed in detail for BT-BNTs by Kunstmann *et al.*[29] For BT-BNT zz nanotubes no clear trend in E^{st} is visible and their energies change only slightly with the diameter. It seems that these structures can be rolled up without significant energy cost.[15,29] A very unusual behavior is found for DH-BNT zz tubes, as their strain energies are negative[11] except for the two with the smallest diameters (see Figure 2b), and reach the minimum value for the (6,−6) DH-BNT zz nanotube (which is the most stable one). This means that the DH boron sheet gains energy by rolling up along its zigzag direction and that the DH-BNT zz tubes with diameter close to 0.4 nm are particularly stable. We ascribe this behavior to the undercoordination of boron atoms in the DH sheet. In stable phases of elemental boron, the coordination numbers range from 4 to 7, but the majority of the atoms are always 6-fold coordinated.[30] In the DH boron sheet, the atoms are apparently only 3-fold coordinated. However, the bond length to the second-nearest neighbor along the zigzag chains (see Figure 1c) is 2.00 Å in the sheet, reaches 1.97 Å in the most stable (6,−6) DH-BNT zz nanotube, and is equal to 1.99 Å for the smallest (3,−3) DH-BNT zz structure. Among all bond lengths, the second-nearest neighbor

distance is the one that varies the most with the DH zigzag tube diameter. Therefore, rolling up the sheet is a way to shorten and thus strengthen the multicenter bonds in the zigzag chains of the DH sheet and to partly overcome the undercoordination of the atoms. This increases the cohesive energy of the zigzag DH-BNTs with respect to the DH sheet. However, this effect is counterbalanced by changes of other bond lengths. The (6,−6) DH-BNT zz nanotube seems to be the system where this mechanism works best, and therefore it is the most stable nanotube of the DH structural class.

Our results indicate that boron's well-known polymorphism is particularly complex for small-diameter ($D < 2$ nm) BNTs. The nanotubes derived from the three considered structural classes compete, and the relative structural stability is strongly diameter-dependent. For BNTs with a diameter of about 0.5 nm the α-BNTs, DH-BNT zz, and BT-BNT zz are all very close in energy and a particularly strong polymorphism is to be expected. Our findings for very small diameter BNTs are relevant for the ongoing discussion about the structural evolution of BNTs from small boron clusters. It was experimentally observed that a B_{20} cluster is the smallest cluster with a tubular shape. This finding was theoretically confirmed by showing that other potential morphologies of the B_{20} cluster are less stable.[8,9,31] In our notation the B_{20} cluster corresponds to a single unit cell (a double-ring) of a (0,10) BT-BNT arm nanotube with a diameter of 0.52 nm. However, our results in Figure 2a indicate that BT-BNT arm nanotubes with such small diameters are the most unfavorable structures. This strikingly different behavior is very surprising and stems from the fact that we are considering infinite nanotubes while the B_{20} cluster is a finite size object. This indicates that the B_{20} cluster is probably not the embryo of BNTs as suggested by Kiran *et al.*,[9] because if a BNT grew from a B_{20} cluster along the axial direction, the resulting BT-BNT arm would be energetically unfavorable compared to other structures.

Work Functions. After comparing the diameter-dependent stability of different BNTs we now want to find out if the physical properties derived from BNTs of the three structural classes can be compared to recently measured transport properties and work functions.[1]

The nanotubes in the experiments of Liu *et al.*[1] are multiwalled nanotubes with large diameters of about 10 to 40 nm, with a spacing between adjacent boron layers of about 3.2 Å. We model this situation by studying single-walled BNTs with $D \approx 10$ nm, which can be considered as the outermost walls of multiwalled BNTs. For a BNT of that size the quantum confinement and curvature effects are small and the nanotube's physical properties are very similar to the properties of a single boron sheet. Therefore the measured work functions of BNTs can be directly compared to the work functions of the boron sheets as done in Table 1.[32]

TABLE 1. Calculated and Experimentally Measured Work Functions of Graphene and Boron Sheets (in eV)[a]

	calculation	experiment
graphene	4.60	4.66[33]
α-sheet	4.09	4.02[1]
BT-sheet	5.39	
DH-sheet	4.89	

[a] The experimental value for boron structures was obtained from a mixed film of large-diameter boron nanotubes and boron nanowires, and it compares well to the theoretical value for the α-sheet. A comparison between sheets and nanotubes is possible because the nanotubes have large diameters. The excellent agreement between experiment and calculation is indirect evidence for the existence of α-sheet nanotubes.

The work functions were calculated with DFT/PBE[24] from the difference between the vacuum level (the potential at the large distance from the sheet) and the Fermi energy.[32] As a test case, we calculated the work function of graphene and obtained 4.60 eV, which is very close to the experimental value of 4.66 eV.[33] This demonstrates the reliability of the chosen numerical approach. The comparison between experiment and theory in Table 1 shows that the experimental value measured by Liu *et al.*[1] for a mixed film of boron nanotubes and boron nanowires (4.02 eV) agrees well with the calculated value of the α-sheet (4.09 eV). To interpret this finding let us consider that the work function measured for a mixture of two nanostructured materials is close to the smallest work function of the constituents. As the work function measured for pure boron nanowires is 4.52 eV,[1] that of BNTs will be close to 4.02 eV. The work functions calculated for the BT sheet and the DH sheet (5.39 and 4.89 eV, respectively) are noticeably higher than the work function measured for boron nanowires. Therefore the only known structure that fits with the experiment is the α-sheet. This finding can be considered as an indirect evidence that the atomic structure of boron nanotubes is related to the α-sheet.

Electronic Structure and Electron Transport. In the following we study the electronic structure and the intrinsic transport properties of BNTs. First, the electronic structures of BNTs with diameters of approximately 10 nm are calculated. We consider one armchair and one zigzag BNT of each structural class. These are (64,0) α-BNT arm, (36,36) α-BNT zz, (0,200) BT-BNT arm, (110,0) BT-BNT zz, (54,54) DH-BNT arm, and (160,−160) DH-BNT zz having diameters of 10.2, 9.9, 10.3, 10.0, 10.2, and 10.2 nm, respectively (see Supporting Information for the description of the (*n*,*m*) nomenclature and the geometries). Calculations of such large nanotubes are unfeasible with standard DFT methods. Therefore we use the density functional tight-binding method (DFTB).[34] The corresponding

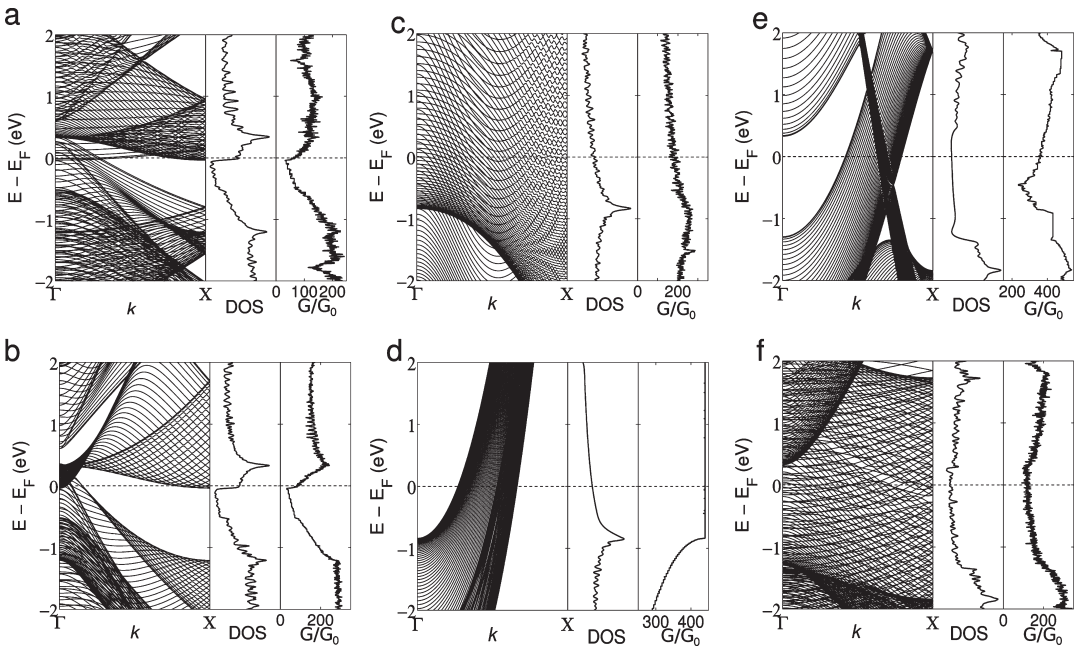

Figure 3. Electronic structures of armchair (first row) and zigzag boron nanotubes (second row) with diameters of about 10 nm. Each panel shows the band structure, the density of states (DOS), and the conductance profile $G(E)/G_0$ for the maximum conductance. The first, second, and third column correspond to boron nanotubes of the α, buckled triangular (BT), and distorted hexagonal (DH) types, respectively (in detail: [a] (64,0) α-BNT arm, [b] (36,36) α-BNT zz, [c] (0,200) BT-BNT arm, [d] (110,0) BT-BNT zz, [e] (54,54) DH-BNT arm, and [f] (160,−160) DH-BNT zz). All BNTs are metallic (they have a finite DOS at the Fermi energy, E_F) and highly conductive (as a large number of conduction channels G/G_0 are available). α-BNTs have a wide dip in the DOS and in G close to the Fermi energy, which is reflected in the corresponding current−voltage characteristics in Figure 5.

band structures, density of states (DOS), and conductance profiles $G(E)/G_0$ ($G_0 = e^2/h$ is the conductance quantum) for zero bias are shown in Figure 3. The conductance profiles $G(E)$ reflect the maximal intrinsic conductance of an ideal BNT. Structural imperfections like defects, impurities, adatoms, *etc.*, will lower the conductance.

As can be seen from this figure, all BNTs are metallic since they have no band gap at the Fermi energy E_F. The fact that BNTs are generally metallic, irrespective of their structural class, diameter, or chirality is well known[10,11,15,18] and is confirmed by our results.

As already mentioned above, the quantum confinement effects on the electronic structure for large-diameter nanotubes are almost negligible and the system is quite similar to the sheet. This effect is illustrated in Figure 4, where the band structures, the DOS, and the conductance profiles of two metallic CNTs [(74,74) and (129,0)] with diameters of 10.0 and 10.1 nm, respectively, are presented. The band structures are a quantized version of the one of graphene. They clearly show the well-known touching cones with a nearly vanishing DOS at E_F and a linear increase in the DOS near E_F. Furthermore the conductance profiles of the two nanotubes are almost identical; this holds for all metallic CNTs of similar diameters. For the BNTs in Figure 3 this size effect is reflected in the fact that the DOS of armchair and zigzag BNTs and the boron sheet for one structural class are all very similar (see Supporting

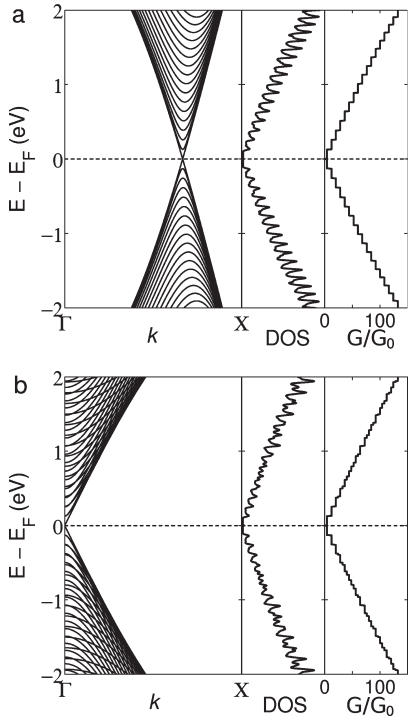

Figure 4. Electronic structures of (a) a (74,74) armchair and (b) a (129,0) zigzag carbon nanotube with diameters of 10.0 and 10.1 nm, respectively. Each panel shows the band structure, the density of states (DOS), and the conductance profile $G(E)/G_0$ for the maximum conductance. Due to their large diameters the electronic properties of the CNTs are very similar to the properties of graphene. The conductance profiles of the two nanotubes are virtually identical.

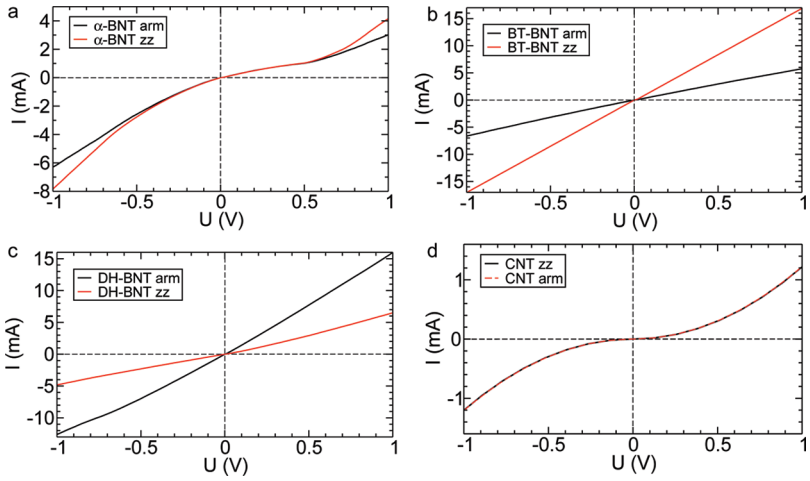

Figure 5. Current−voltage characteristics of armchair and zigzag boron nanotubes and carbon nanotubes with diameters of about 10 nm. The nearly flat conductance profiles of buckled triangular and distorted hexagonal boron nanotubes (see Figure 3) lead to almost linear *I*−*U* curves, whereas the pronounced dips in the conductance profiles of the α-BNTs and the carbon nanotubes result in nonlinear *I*−*U* curves. The *I*−*U* curves of boron nanotubes of one structural class agree qualitatively, but they are chirality dependent on a quantitative level. The two metallic carbon nanotubes, on the other hand, have identical *I*−*U* curves.

Information for the DOS of the three boron sheets). The size effect and the above arguments also apply to the conductance profiles $G(E)$ of all nanotubes (see Figure 3). Generally we find that all BNTs have about 1−2 orders of magnitude more conductance channels near E_F than the metallic CNTs (which have only 4 channels, including spin degeneracy). This shows that BNTs are highly conductive and are much better conductors than CNTs.

The DOS and the conductance profiles of the α-BNTs (as well as the α-sheet) exhibit a pronounced dip with an energy width of ca. 1.5 eV near E_F . This dip corresponds to the band gap of in-plane states, separating the in-plane bonding states from the antibonding ones, as shown by Tang *et al.*[12] The remaining states near E_F are out-of-plane (p_z) states. The BT and DH systems do not have such a well-defined characteristic feature; instead their DOS and the conductance profiles are nearly flat near E_F. These features are reflected in the current−voltage characteristics of the BNTs.

The current−voltage characteristics for small voltages ($|U| < 1$ V) are calculated with the Landauer−Büttiker formalism[35,36] from the conductance profiles. In the experiments the BNTs are grown on a silicon substrate and are contacted by a tungsten tip.[1] As the tungsten tip touches the outer wall of a multiwalled BNT, the current is defined mainly by the electrons transmitted through the outer tube, which is represented by the single-wall BNTs studied here. For the calculation of the current we assume transparent contacts and model the silicon and tungsten contacts by their work functions (see Methods section). This approach corresponds to an idealized situation, and the resulting currents can be interpreted as maximum currents that can be transmitted through a BNT *via* ballistic transport.

The calculated current−voltage curves are presented in Figure 5. All BNTs show metallic behavior in agreement with the experimental results. The currents of all BNTs are higher than the current transmitted through CNTs of similar size. This stems from the fact that the BNTs have more conduction channels close to Fermi energy than the CNTs. However, the currents of BNTs and CNTs in the bias range of $|U| < 1$ V are all of the same order of magnitude, *i.e.*, a few milliamperes. These rather large currents are reached because the large-diameter tubes have a few hundred conduction channels. A comparison with the measured *I*−*U* curves of Liu *et al.*[1] shows that the calculated currents are about 4 orders of magnitude higher than the measured ones. This large difference shows that our theoretical transport model does not match the experimental conditions well. The effects of resistive (nontransparent) contacts[37] and the influence of structural imperfection of the BNTs probably have to be taken into account. It could also be that none of the structural models of the BNTs that we are considering are correct. In any case a better experimental characterization of the BNTs would be desirable to proceed further.

Nevertheless, our results reflect the intrinsic properties of BNTs and their potential performance in the case of ideal measurements. The nearly flat conductance profiles of BT- and DH-BNTs (see Figure 3) lead to almost linear *I*−*U* curves, whereas the pronounced dips in the conductance profiles of the α-BNTs and the carbon nanotubes result in nonlinear *I*−*U* curves. The qualitative *I*−*U* behavior of the BNTs of different chiralities within each structural class is similar, as the conductance profiles of large-diameter BNTs within each class are similar (see discussion above). However, on a quantitative level the currents are different, showing that the chirality clearly has an influence on the ballistic current. This is again in contrast to CNTs, where for small voltages all metallic CNTs of similar

radii have identical $I-U$ curves; that is, the two curves in Figure 5d coincide because their conductance profiles are almost identical.

Finally let us bring together all our results and discuss the problem of the determination of the atomic structure of BNTs. Liu *et al.*[1] have argued that the polygonal morphology of the open end of the nanotube shown in high-resolution TEM images corresponds nicely to the faceted surfaces of BNTs obtained by rolling the buckled triangular boron sheet. On the other hand our calculations show that for large diameters the α-BNTs are by far the most stable structures (see Figure 2a). Moreover, the calculated work function of α-BNTs (4.09 eV) is much closer to the experimentally obtained value (4.02 eV) than that of BT-BNTs (5.39 eV). Based on the transport properties of BNTs presented in the current paper, further arguments in favor of one or another type of BNTs can be obtained by the measurement of the current−voltage characteristics of the grown BNTs for small applied voltages (up to 1 V): if all $I-U$ curves would show nonlinearity, it could be argued that they are obtained from BNTs with an atomic structure similar to that of the α-sheet, whereas linear behavior of the curves would correspond to the BT or DH BNTs.

CONCLUSIONS

The intrinsic transport properties of ideal BNTs of three different underlying lattice structures and with diameters of about 10 nm were investigated in the ballistic regime. It was shown that all three types of BNTs have metallic conductivities, irrespective of their diameters and chiralities, which agrees with earlier predictions and recent experiments. A comparison of the current−voltage characteristics ($I-U$ curves) of BNTs to those of metallic CNTs of similar diameters showed that BNTs have higher conductivities since they have significantly more conduction channels close to the Fermi energy. The nearly flat conductance profiles of buckled triangular and distorted hexagonal BNTs lead to almost linear $I-U$ curves, whereas the pronounced dips in the conductance profiles of the α-BNTs result in nonlinear $I-U$ curves. This nonlinearity could allow the distinction of the α-BNTs from the two other types in future experiments. The $I-U$ curves of BNTs within each structural class agree qualitatively, but they are chirality dependent on a quantitative level. This is in contrast to CNTs where *metallic* nanotubes of similar diameters have identical $I-U$ curves independent of the chirality.

Furthermore, it was found that the work function calculated for the α-BNTs is much closer to the experimental value than those of buckled triangular and distorted hexagonal BNTs. This indirectly shows that the atomic structure of boron nanotubes is related to the α-sheet.

The structural stability of nanotubes with diameters less than 2.3 nm was studied. It was found that the stability of BNTs with diameters > 2 nm approaches that of the corresponding boron sheets and that large-diameter α-sheet nanotubes are the most stable ones. However, for smaller diameters the relative stabilities change significantly, and for diameters < 0.5 nm zigzag nanotubes of the buckled triangular sheet are the most stable structures. For structures related to the distorted hexagonal sheet, the most stable nanotube was discovered to be that with a diameter of 0.39 nm. Furthermore, the curvature energy of a boron nanotube depends on both diameter and chirality, except for nanotubes from an α-sheet, where it depends only on the diameter.

METHODS

Ab initio calculations of the structural stability and the work functions of boron sheets, small-diameter boron nanotubes, and graphene were performed with density functional theory within the generalized gradient approximation[24] using the projector-augmented wave method as implemented in the VASP package.[38,39] Full geometry optimizations have been carried out, and the atomic forces were reduced to be below 1 meV/Å. For all these calculations the energy convergence over the number of k points was reached, and the tetrahedron method for k-integration was used.

Electronic structure calculations for large-diameter BNTs were done with the density functional based tight-binding method[34] and the DFTB$^+$ code.[40] For BNTs a newly developed parametrization for boron was used (Grundkötter-Stock, B.; Bezugly, V.; Kunstmann, J.; Cuniberti, G.; Frauenheim, T.; Niehaus, T., in preparation). Self-consistent charge (SCC) calculations for periodic structures were performed with the SCC tolerance set to 10^{-5}, and the electron temperature was kept equal to zero. The energy was converged with respect to the number of k points. The atomic positions for the DFTB calculations correspond to ideal DFT/PBE geometries; that is, we use boron sheets that are optimized with DFT/PBE calculations and then geometrically roll up the sheets into tubes. No further geometry optimizations within DFTB are performed because the possible geometry changes for such curvatures of nanotube walls and the influence of these changes on the electronic structure and transport properties are negligible.[41]

The electronic structures of large-diameter carbon nanotubes were calculated analytically by a first-nearest-neighbor tight-binding model of the π-bands[42] using a transfer integral, overlap integral, and graphene lattice constant of $t_\pi = -3.033$ eV, $s_\pi = 0$, and $a = 2.46$ Å, respectively.

The conductance profile, $G(E)$, is calculated for zero bias by assuming transparent contacts to electrodes (no contact resistance). It is obtained from the corresponding band structure as the number of electronic bands for particular energy multiplied by 2 (for two spin channels) and the conductance quantum G_0. The current along the nanotube (for zero temperature) is calculated within the Landauer−Büttiker formalism[35,36] as

$$I = e^{-1} \int_{\mu_{Si}+\Delta\mu_1}^{\mu_{Si}+\Delta\mu_2} dE\, G(E)$$

where e is the electron charge, μ_{Si} is the chemical potential of the silicon contact, and $\Delta\mu_1 = 0$ eV, $\Delta\mu_2 = U$ for $U > 0$; $\Delta\mu_1 = U$, $\Delta\mu_1 = 0$ eV for $U < 0$, and U is the bias voltage. For this calculation the chemical potential of the silicon contact is taken as the reference (zero bias) and is kept fixed (grounded contact) while varying the chemical potential at the other contact (the tungsten tip). To find the relative position of Fermi

levels of silicon and large-diameter BNTs and CNTs, the work functions of the corresponding two-dimensional sheets were used. The work function of silicon is 4.60 eV.[43]

Acknowledgment. Fruitful discussions with M. H. Rümmeli (IFW Dresden) and C. Toher (TU Dresden) are gratefully acknowledged. We thank D. Nozaki (TU Dresden) for designing the picture for the graphical abstract. V.B. and J.K. acknowledge financial support from the DFG (project KU 2347/2-1). We also acknowledge the Center for Information Services and High Performance Computing (ZIH) at the Dresden University of Technology for computational resources. B.G.-S. and T.N. thank the University of Bremen (ZF 01/120/06) for financial support. G.C. acknowledges support from the South Korean Ministry of Education, Science, and Technology Program, Project WCU ITCE No. R31-2008-000-10100-0.

Supporting Information Available: Details on the lattice structures of boron sheets and boron nanotubes as well as the electronic structures of boron sheets. This material is available free of charge *via* the Internet at http://pubs.acs.org.

REFERENCES AND NOTES

1. Liu, F.; Shen, C.; Su, Z.; Ding, X.; Deng, S.; Chen, J.; Xu, N.; Gao, H. Metal-Like Single Crystalline Boron Nanotubes: Synthesis and *In Situ* Study on Electric Transport and Field Emission Properties. *J. Mater. Chem.* **2010**, *20*, 2197–2205.
2. Baughman, R. H.; Zakhidov, A. A.; de Heer, W. A. Carbon Nanotubes—the Route Toward Applications. *Science* **2002**, *297*, 787–792.
3. Geim, A. Graphene: Status and Prospects. *Science* **2009**, *324*, 1530–1534.
4. Oganov, A. R.; Chen, J.; Gatti, C.; Ma, Y.-Z.; Ma, Y.-M.; Glass, C. W.; Liu, Z.; Yu, T.; Kurakevych, O. O.; Solozhenko, V. L. Ionic High-Pressure Form of Elemental Boron. *Nature* **2009**, *457*, 863–867.
5. Boustani, I. New Quasi-Planar Surfaces of Bare Boron. *Surf. Sci.* **1997**, *370*, 355–363.
6. Boustani, I.; Quandt, A. Nanotubules of Bare Boron Clusters: *Ab Initio* and Density Functional Study. *Europhys. Lett.* **1997**, *39*, 527–532.
7. Zhai, H.-J.; Kiran, B.; Li, J.; Wang, L.-S. Hydrocarbon Analogues of Boron Clusters—Planarity, Aromaticity and Antiaromaticity. *Nat. Mater.* **2003**, *2*, 827–833.
8. Oger, E.; Crawford, N. R. M.; Kelting, R.; Weis, P.; Kappes, M. M.; Ahlrichs, R. Boron Cluster Cations: Transition from Planar to Cylindrical Structures. *Angew. Chem., Int. Ed.* **2007**, *46*, 8503–8506.
9. Kiran, B.; Bulusu, S.; Zhai, H.-J.; Yoo, S.; Zeng, X. C.; Wang, L.-S. Planar-To-Tubular Structural Transition in Boron Clusters: B20 As the Embryo of Single-Walled Boron Nanotubes. *Proc. Natl. Acad. Sci. U. S. A.* **2005**, *102*, 961–964.
10. Boustani, I.; Quandt, A.; Hernandez, E.; Rubio, A. New Boron Based Nanostructured Materials. *J. Chem. Phys.* **1999**, *110*, 3176–3185.
11. Lau, K. C.; Pati, R.; Pandey, R.; Pineda, A. C. First-Principles Study of the Stability and Electronic Properties of Sheets and Nanotubes of Elemental Boron. *Chem. Phys. Lett.* **2006**, *418*, 549–554.
12. Tang, H.; Ismail-Beigi, S. Novel Precursors for Boron Nanotubes: The Competition of Two-Center and Three-Center Bonding in Boron Sheets. *Phys. Rev. Lett.* **2007**, *99*, 115501—1–4.
13. Singh, A. K.; Sadrzadeh, A.; Yakobson, B. I. Probing Properties of Boron α-Tubes by *Ab Initio* Calculations. *Nano Lett.* **2008**, *8*, 1314–1317.
14. Yang, X.; Ding, Y.; Ni, J. Ab Initio Prediction of Stable Boron Sheets and Boron Nanotubes: Structure, Stability, and Electronic Properties. *Phys. Rev. B* **2008**, *77*, 041402(R)-1–4.
15. Kunstmann, J.; Quandt, A. Broad Boron Sheets and Boron Nanotubes: An *Ab Initio* Study of Structural, Electronic, and Mechanical Properties. *Phys. Rev. B* **2006**, *74*, 035413—1–14.
16. Ciuparu, D.; Klie, R. F.; Zhu, Y.; Pfefferle, L. Synthesis of Pure Boron Single-Wall Nanotubes. *J. Phys. Chem. B* **2004**, *108*, 3967–3969.
17. Lau, K. C.; Pandey, R. Thermodynamic Stability of Novel Boron Sheet Configurations. *J. Phys. Chem. B* **2008**, *112*, 10217–10220.
18. Szwacki, N. G.; Tymczak, C. J. The Symmetry of the Boron Buckyball and a Related Boron Nanotube. *Chem. Phys. Lett.* **2010**, *494*, 80–83.
19. He, H; Pandey, R.; Boustani, I.; Karna, S. P. Metal-like Electrical Conductance in Boron Fullerenes. *J. Phys. Chem. C* **2010**, *114*, 4149–4152.
20. Li, G. Q. The Transport Properties of Boron Nanostructures. *Appl. Phys. Lett.* **2009**, *94*, 193116-1–3.
21. Li, G. Q. *Ab Initio* Investigation of Boron Nanodevices: Conductances of the Different Geometric Conformations. *Chin. Phys. B* **2010**, *19*, 017201-1–5.
22. Lau, K. C.; Pandey, R.; Pati, R.; Karna, S. P. Theoretical Study of Electron Transport in Boron Nanotubes. *Appl. Phys. Lett.* **2006**, *88*, 212111-1–3.
23. Guo, W.; Hu, Y.-B.; Zhang, Y.-Y.; Du, S.-X.; Gao, H.-J. Transport Properties of Boron Nanotubes Investigated by *Ab Initio* Calculation. *Chin. Phys. B* **2009**, *18*, 2502–2506.
24. Perdew, J. P.; Burke, K.; Ernzerhof, M. Generalized Gradient Approximation Made Simple. *Phys. Rev. Lett.* **1996**, *77*, 3865–3868.
25. Zhang, D.; Zhu, R.; Liu, C. Density Functional Theory Study on the Geometrical and Electronic Structures of a New Thinnest Boron Nanotube. *J. Mater. Chem.* **2006**, *16*, 2429–2433.
26. Boustani, I.; Quandt, A.; Kramer, P. Tubular Structures in Alpha-Rhomboedral Quasicrystals. *Europhys. Lett.* **1996**, *36*, 583–588.
27. Chacko, S.; Kanhere, D. G.; Boustani, I. Ab Initio Density Functional Investigation of B_{24} Clusters: Rings, Tubes, Planes and Cages. *Phys. Rev. B* **2003**, *68*, 035414-1–11.
28. Robertson, D. H.; Brenner, D. W.; Mintmire, J. W. Energetics of Nanoscale Graphitic Tubules. *Phys. Rev. B* **1992**, *45*, 12592–12595.
29. Kunstmann, J.; Quandt, A.; Boustani, I. An Approach To Control the Radius and the Chirality of Nanotubes. *Nanotechnology* **2007**, *18*, 155703-1–3.
30. Hoard, J. L.; Hughes, R. E. Elemental Boron and Compounds of High Boron Content: Structure, Properties, and Polymorphism. In *The Chemistry of Boron and its Compounds*; Muetterties, L., Ed.; John Wiley & Sons: New York, 1967; pp 25—154.
31. Özdogan, C.; Mukhopadhyay, S.; Hayami, W.; Guvenc, Z. B.; Pandey, R.; Boustani, I. The Unusually Stable B100 Fullerene, Structural Transitions in Boron Nanostructures, and a Comparative Study of α- and γ-Boron and Sheets. *J. Phys. Chem. C* **2010**, *114*, 4362–4375.
32. Shan, B.; Cho, K. First Principles Study of Work Functions of Single Wall Carbon Nanotubes. *Phys. Rev. Lett.* **2005**, *94*, 236602-1–4.
33. Shi, Y.; Kim, K. K.; Reina, A.; Hofmann, M.; Li, L.-J.; Kong, J. Work Function Engineering of Graphene Electrode *via* Chemical Doping. *ACS Nano* **2010**, *4*, 2689–2694.
34. Elstner, M.; Porezag, D.; Jungnickel, G.; Elsner, J.; Haugk, M.; Frauenheim, T.; Suhai, S.; Seifert, G. Self-Consistent-Charge Density-Functional Tight-Binding Method for Simulations of Complex Materials Properties. *Phys. Rev. B* **1998**, *58*, 7260–7268.
35. Landauer, R. Spatial Variation of Currents and Fields Due To Localized Scatterers in Metallic Conduction. *IBM J. Res. Dev.* **1957**, *1*, 223–231.
36. Büttiker, M. Four-Terminal Phase-Coherent Conductance. *Phys. Rev. Lett.* **1986**, *57*, 1761–1764.
37. Nemec, N.; Tomanek, D.; Cuniberti, G. Modeling Extended Contacts for Nanotube and Graphene Devices. *Phys. Rev. B* **2008**, *77*, 125420-1–12.
38. Kresse, G.; Joubert, D. From Ultrasoft Pseudopotentials to the Projector Augmented-Wave Method. *Phys. Rev. B* **1999**, *59*, 1758–1775.

39. Kresse, G.; Furthmüller, J. Efficient Iterative Schemes for *Ab Initio* Total-Energy Calculations Using a Plane-Wave Basis Set. *Phys. Rev. B* **1996**, *54*, 11169–11186.
40. Aradi, B.; Hourahine, B.; Frauenheim, T. DFTB+, a Sparse Matrix-Based Implementation of the DFTB Method. *J. Phys. Chem. A* **2007**, *111*, 5678–5684.
41. Tang, H.; Ismail-Beigi, S. First-Principles Study of Boron Sheets and Nanotubes. *Phys. Rev. B* **2010**, *82*, 115412–1−20.
42. Saito, R.; Dresselhaus, G.; Dresselhaus, M. S. *Physical Properties of Carbon Nanotubes*. Imperial College Press: London, 2005; pp 26−29, 59−61.
43. *CRC Handbook of Chemistry and Physics*; Lide, D. R., Ed.; CRC Press: Boca Raton, FL, 2008; pp 12−114.